ENHANCING REWEIGHTED LOW-RANK REPRESENTATION FOR HYPERSPECTRAL IMAGE UNMIXING

Wu-Chao Di, Jie Huang*, Jin-Ju Wang, and Ting-Zhu Huang

School of Mathematical Sciences, University of Electronic Science and Technology of China, Chengdu, Sichuan, 611731, PR China.

ABSTRACT

Sparse hyperspectral unmixing has attracted much attention in recent decades. Recently, the low-rank representation provides a new perspective for spatial correlation and the weighted nuclear norm regularization has been well studied to enhance the low-rankness of the abundance matrix. However, the commonly used weights only depend on respective singular values, ignoring other singular values' information. In this paper, we propose a new weighting scheme for the weighed nuclear norm to further enhance the sparsity of the singular values of the abundance matrix. The proposed weight for each singular value considers information of all singular values, instead of particular singular value only. Then we refine two sparsity and low-rankness based unmixing algorithms. Simulated and real-data experiments demonstrate the effectiveness of the resulting unmixing algorithms.

Index Terms— Hyperspectral images, spectral unmixing, abundance estimation, low-rank matrix, weighted nuclear norm.

1. INTRODUCTION

Hyperspectral unmixing (HU) is an important research topic for hyperspectral image analysis. It can be described as a process of recognizing the spectral signatures of materials (endmembers) which consist of the pixels in hyperspectral images (HSIs) and estimating the fractions (abundance) of each pixel [1]. The linear mixture model (LMM) has been widely used in HU. It assumes that each pixel is a mixture of materials in a certain proportion. Sparse HU becomes a hot topic in the past ten years. It assumes that each pixel consists of relatively a few endmembers, compared with available potential large-scale dictionaries, and therefore the resulting abundance matrix has a sparsity property [2, 3].

Recently, the low-rank representation of HSIs provides a new perspective on spatial information for HU. The spatial correlation between each pixel and its neighbors trans-

lates into the linear dependance of the corresponding fractional abundances [4]. It follows that the fractional abundance matrix admits a low-rank property. Simultaneously imposing low rankness and sparsity on the abundance matrix improves the abundance accuracy [5, 6]. Notice that in both alternating direction sparse and low-rank unmixing algorithm (ADSpLRU) [5] and joint-sparse-blocks and low-rank unmixing algorithm (JSpBLRU) [6], the weighted nuclear norm with a reweighting strategy [7] is adopted to enforce the low rankness on the abundance matrix. Specifically, the weights are designed to increase the punishment on smaller singular values and decrease the punishment on large singular values simultaneously. It is shown that the reweighting coefficients improve the unmixing performance greatly. We note that, however, each weight is only dependent on its corresponding singular value and thus ignores potential information from other singular values.

In this paper, we propose a new weighting scheme for the weighted nuclear norm to further promote the low-rankness of the abundance matrix. The main idea is to consider the information from all singular values and further increase the punishment on smaller singular values and decrease the punishment on large singular values simultaneously. Then we refine ADSpLRU and JSpBLRU with the proposed weighting scheme. Simulated and real-data experiments demonstrate the effectiveness of the resulting unmixing algorithms.

2. MODELS AND ALGORITHMS

Let $Y \in \mathbb{R}^{m \times k}$ be the observed data matrix, where m is the band number and k is the pixel number. Let $A \in \mathbb{R}^{m \times n}$ be the spectral dictionary with n being the endmember number. Then the LMM assumes that

$$Y = AX + E,$$

where $X \in \mathbb{R}^{n \times k}$ is the abundance matrix and $E \in \mathbb{R}^{m \times k}$ is a noise matrix. In addition, the *abundance nonnegative constraint* and *the abundance sum-to-one constraint*, i.e. $X \geq 0$ and $\sum_{i=1}^{n} x_{ij} = 1$, respectively, are two physical constraints.

Recently, the low-rank representation has been studied for sparse HU [4, 5, 6].Specially, simultaneously imposing spar-

sity and low rankness leads to the unmixing model [5]

$$\min_{X \geq 0} \frac{1}{2} \|Y - AX\|_F^2 + \gamma \|W \odot X\|_1 + \tau \|X\|_{f,*}, \quad (1)$$

where γ and τ are nonnegative regularization parameters,

$$\|W \odot X\|_1 = \sum_{i=1}^{n} \sum_{j=1}^{k} |w_{ij} x_{ij}|, \quad \|X\|_{f,*} = \sum_{i=1}^{n} f(\sigma_i)\sigma_i,$$

and σ_i is the i-th singular value of X. Note that $\|X\|_{f,*}$ is the weighted nuclear norm of X and $f(\sigma_i) = 1$ for each i gives the standard nuclear norm $\|X\|_*$. Here, the weighting function f is defined element-wisely as

$$f(x) = \frac{1}{x + \varepsilon}, \quad (2)$$

where $\varepsilon = 10^{-16}$ is a small number to avoid singularities.

In this paper, we propose a new weighting function for the weighted nuclear norm to further enhance the sparsity of the singular values of the abundance matrix. To begin, assume that $k > n$ and $\sigma_1 \geq \sigma_2 \geq \cdots \geq \sigma_n$. In order to consider the information from all singular values, we find the smallest q and corresponding maximum σ_q satisfying

$$\frac{\sum_{i=1}^{q} \sigma_i}{\sum_{i=1}^{n} \sigma_i} \geq p, \quad (3)$$

where $p \in (0, 1]$ is a thresholding parameter. We note that if the rank of X is r, then we hope $\sigma_q = \sigma_r$. With the obtained σ_q, we now define the new weighting function g as

$$g(x) = \frac{1}{x + \varepsilon} \exp(\sigma_q - x). \quad (4)$$

It follows that for each i,

$$g(\sigma_i) = \frac{1}{\sigma_i + \varepsilon} \exp(\sigma_q - \sigma_i). \quad (5)$$

Clearly, we see from Eq. (5) that, comparing with the weighting function f, the function g further decreases the punishment on the first q singular values and increases the punishment on other singular values. In other words, larger singular values are assigned smaller weights and smaller singular values are assigned larger weights. To further compare the two weighting functions f and g, we show their curves in Fig. 1. Then from the figure, we see that $f(x) < g(x)$ for $x < \sigma_q$, $f(x) > g(x)$ for $x > \sigma_q$, and $f(\sigma_q) = g(\sigma_q)$. Clearly, the curves are consistent with the previous observation.

We now refine two unmixing models by replacing the weighting function f with the proposed weighting function g for the weighted nuclear norm in (1) and in the JSpBLRU model [6], respectively. They are

$$\min_{X \geq 0} \frac{1}{2} \|Y - AX\|_F^2 + \gamma \|W_1 \odot X\|_1 + \tau \|X\|_{g,*}, \quad (6)$$
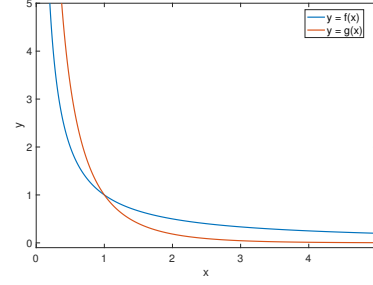

Fig. 1. Curves of the weighting functions f in (2) and g with $\sigma_q = 1$ in (4).

and

$$\min_{X \geq 0} \frac{1}{2} \|Y - AX\|_F^2 + \gamma \sum_{j=1}^{s} \|X_j\|_{W_2,2,1} + \tau \|X\|_{g,*}, \quad (7)$$

where $\|X\|_{g,*} = \sum_{i=1}^{n} g(\sigma_i) \sigma_i$, $X = [X_1, X_2, \ldots, X_s]$, and $\|X_j\|_{W_2,2,1}$ is the weighted $\ell_{2,1}$-norm of X_j. Similarly as in [5, 6], we solve the above two models by the alternating direction method of multipliers (ADMM).

Take for example the model in (6). First, we equivalently transform (6) into a constrained problem

$$\min_{X} \frac{1}{2} \|Y - V_1\|_F^2 + \gamma \|W_1 \odot V_2\|_1 + \tau \|V_3\|_{g,*} + \iota_{R_+}(V_4)$$

$$\text{s.t.} \quad V_1 = AX, \; V_2 = X, \; V_3 = X, \; V_4 = X,$$

where $\iota_{R_+}(x)$ is the indicator function, i.e., $\iota_{R_+}(x) = 0$ if x is nonnegative and $\iota_{R_+}(x) = +\infty$ otherwise. Define

$$\mathcal{L}(X, V; D) = \frac{1}{2} \|Y - V_1\|_F^2 + \gamma \|W_1 \odot V_2\|_1$$

$$+ \tau \|V_3\|_{g,*} + \iota_{R_+}(V_4) + \frac{\mu}{2} \|GX + BV - D\|_F^2,$$

where $V = [V_1^T, V_2^T, V_3^T, V_4^T]^T$, $D = [D_1^T, D_2^T, D_3^T, D_4^T]^T$ is the Lagrange multiplier, $B = \text{diag}(-I, -I, -I, -I)$, $G = [A^T, I, I, I]^T$, and $\mu > 0$. Then the ADMM framework is

$$\begin{cases} X^{k+1} = \underset{X}{\text{argmin}} \, \mathcal{L}(X, V^k; D^k), \\ V^{k+1} = \underset{V}{\text{argmin}} \, \mathcal{L}(X^{k+1}, V; D^k), \\ D^{k+1} = D^k - (GX^{k+1} + BV^{k+1}). \end{cases}$$

To make the notations concisely, we give the soft-thresholding (SHR) operator and the singular value thresholding (SVT) operator. Let $X = U\Sigma V^T$ be the singular value decomposition of X and recall the functions in (2) and (4), then we define:

$$\text{SHR}_{f,\alpha}(x) = \text{sign}(x) \max(0, x - \alpha f(x)),$$

$$\text{SVT}_{g,\beta}(X) = U \text{SHR}_{g,\beta}(\Sigma) V^T.$$

Now we give the proposed algorithm, named as the *alternating direction sparse and enhancing low-rank* unmixing algorithm (ADSpEnLRU) in the following.

3826

Algorithm 1: ADSpEnLRU

Input: Y, A.

Selected parameters: μ, τ, γ

Initialization: D^0, V^0, and $t = 1$

Repeat:

$$X^t = \left(A^T A + 3I\right)^{-1}\left(A^T\left(D_1^{t-1} + V_1^{t-1}\right) + D_2^{t-1} + \right.$$
$$\left. V_2^{t-1} + V_3^{t-1} + D_3^{t-1} + V_4^{t-1} + D_4^{t-1}\right)$$
$$V_1^t = 1/\left(1+\mu\right)\left(Y + \mu\left(AX^t - D_1^{t-1}\right)\right)$$
$$V_2^t = \mathrm{SHR}_{f,\frac{\gamma}{\mu}}\left(X^t - D_2^{t-1}\right)$$
$$V_3^t = \mathrm{SVT}_{g,\frac{\tau}{\mu}}\left(X^t - D_3^{t-1}\right)$$
$$V_4^t = \max(X^t - D_4^{t-1}, 0)$$
$$D_1^t = D_1^{t-1} - AX^t + V_1^t$$
$$D_i^t = D_i^{t-1} - X^t + V_i^t, \text{ for } i = 2, 3, 4$$

until some stopping criterion is met.

Output: $\hat{X} = X^t$

Similarly, we solve the model in (7) under ADMM and call the resulting algorithm as the *joint-sparse-blocks and enhancing low-rank* unmixing algorithm (JSpBEnLRU). Here we omit the details due to the space consideration.

3. EXPERIMENTS

In this section, we test the performance of SUnSAL [2], CLSUnSAL [3], SUnSAL-TV [8], ADSpLRU [5], AD-SpEnLRU, JSpBLRU [6], and JSpBEnLRU on both simulated and real data.

3.1. Experiment on simulated data

In this example, the spectral dictionary A consists of 120 materials and 99 spectral bands. It is from the National Aeronautics and Space Administration Johnson Space Center Spacecraft Materials Spectral Database. Nine signatures are first randomly chosen from A and then used to generate a 100×100-pixel data cube according to LMM. The generated data is contaminated by Gaussian noise with the signal-to-noise ratio (SNR) of 20, 30, and 40 dB. Similarly as in [5, 6], we use the root-mean-square error (RMSE) and the signal-reconstruction error (SRE) to measure the estimated abundance matrix. They are defined as,

$$\mathrm{RMSE} = \sqrt{\frac{1}{mn}\sum_{i=1}^{n}\|\hat{\mathrm{x}}_i - \mathrm{x}_i\|_2^2}, \ \mathrm{SRE} = 10\log_{10}\left(\frac{\sum_{i=1}^{n}\|\mathrm{x}_i\|_2^2}{\sum_{i=1}^{n}\|\hat{\mathrm{x}}_i - \mathrm{x}_i\|_2^2}\right),$$

respectively, where $\hat{\mathrm{x}}_i$ and x_i are the estimated and true abundance vectors of the ith pixel. Generally speaking, lower RMSEs and higher SREs give better estimations. The stopping criterion of ADSEnLRU and JSpBEnLRU is similar to that of ADSpLRU and JSpBLRU. Here we set $p = 0.7$ and 0.6 in (3) for ADSpEnLRU and JSpBEnLRU, respectively.

Table 1 shows the SRE and RMSE values by different unmixing algorithms. We see that the SREs and RMSEs

Table 1. SRE(dB) and RMSE by different unmixing algorithms when the simulated observations are corrupted by gaussian noise.

Algorithm	SNR = 20 dB		SNR = 30 dB		SNR = 40 dB	
	SRE	RMSE	SRE	RMSE	SRE	RMSE
SUnSAL	3.33	0.0494	8.29	0.0279	13.84	0.0147
CLSUnSAL	2.39	0.0550	5.64	0.0379	11.10	0.0202
SUnSAL-TV	8.21	0.0281	13.36	0.0156	19.81	0.0074
ADSpLRU	7.66	0.0300	16.91	0.0103	26.34	0.0035
ADSpEnLRU	8.06	0.0286	17.34	0.0098	26.43	0.0034
JSpBLRU	9.98	0.0230	18.94	0.0082	28.60	**0.0027**
JSpBEnLRU	**10.25**	**0.0223**	**19.10**	**0.0080**	**28.67**	**0.0027**

provided by SUnSAL and CLSUnSAL with only one regularization term are poorer than those provided by other algorithms with two regularization terms. SUnSAL-TV provides better results. JSpBEnLRU and ADSpEnLRU outperform the original JSpBLRU and ADSpLRU, respectively. Clearly, JSpBEnLRU provides best results. For further comparison, we show estimated abundance maps for endmember #7 by different algorithms in Fig. 2. It shows that SUnSAL and CLSUnSAL produce estimations with less accuracy. SUnSAL-TV gives relatively over-smooth result as expected. Clearly, JSpBEnLRU simultaneously delineates high fractional abundance regions with better accuracy and provides smoother background.
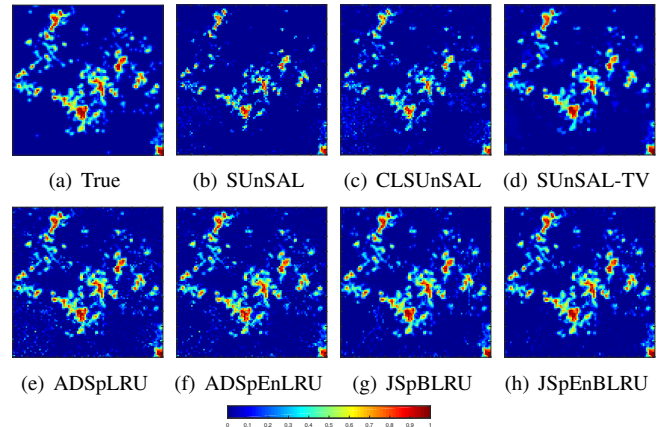

(a) True	(b) SUnSAL	(c) CLSUnSAL	(d) SUnSAL-TV

(e) ADSpLRU	(f) ADSpEnLRU	(g) JSpBLRU	(h) JSpEnBLRU

Fig. 2. True and estimated abundance maps for endmembers #7 by different unmixing algorithms for the simulated data with SNR = 30 dB.

To demonstrate the effectiveness of the proposed reweighting function for the weighted nuclear norm for HU problems, we show the first 16 singular values of the true abundance matrix and its estimations by ADSpLRU and ADSpEnLRU in Fig. 3. We see that both ADSpLRU and ADSpEnLRU provide close results for larger singular values. However, the obtained singular values by ADSpEnLRU vanish faster, showing the better sparsity of the singular values.
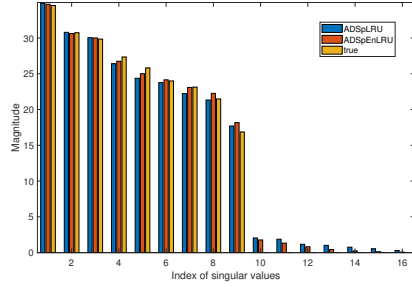
Fig. 3. The first 16 singular values of the true abundance matrix with rank 9 and estimations by ADSpLRU and AD-SpEnLRU for the simulated data with SNR = 20 dB.
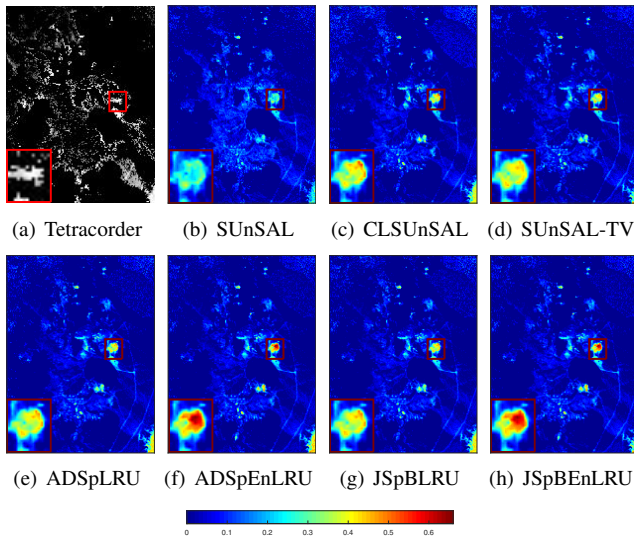

(a) Tetracorder (b) SUnSAL (c) CLSUnSAL (d) SUnSAL-TV

(e) ADSpLRU (f) ADSpEnLRU (g) JSpBLRU (h) JSpBEnLRU

Fig. 4. Estimated abundance maps for *Montmorillonite* by different unmixing algorithms.

3.2. Experiment on real data

In this test, we illustrate the performance of ADSpEnLRU and JSpBEnLRU on the well-known Airborne Visible/Infrared Imaging Spectrometer (AVIRIS) Cuprite data set[1]. We use a subscene of the Cuprite data with 200×150 pixels and 188 spectral bands. The spectral dictionary A of size 188×240 is generated from the U.S. Geological Survey spectral library[2].

Fig. 4 shows the abundance maps for *Montmorillonite* estimated by Tetracorder and different unmixing algorithms. We see from Fig. 4 that all algorithms produce overall similar abundance maps. It may partially due to the low noise level of the Cuprite data. Nevertheless, the fractional abundances estimated by ADEnSpLRU and JSpBEnLRU are generally comparable or higher in the considered regions, verifying the effectiveness of our approach.

---

[1] Available online: http://aviris.jpl.nasa.gov/html/aviris.freedata.html

[2] Available online: http://speclab.cr.usgs.gov/spectral.lib06

4. CONCLUSION

In this paper, we have proposed a new weighting function for the weighted nuclear norm for the HU problem. The weighting strategy aims at increasing the punishment on smaller singular values and decreasing the punishment on larger singular values. With the proposed weighting function, we refine AD-SpLRU and JSpBLRU and term the resulting algorithms as ADSpEnLRU and JSpBEnLRU, respectively. Both simulated and real-data experiments show that the refined unmixing algorithms provide abundance estimations with better or comparable accuracy.

5. REFERENCES

[1] J. Bioucas-Dias, A. Plaza, N. Dobigeon, M. Parente, Q. Du, P. Gader, and J. Chanussot, "Hyperspectral unmixing overview: Geometrical, statistical, and sparse regression-based approaches," *IEEE J. Sel. Topics Appl. Earth Observ. Remote Sens.*, vol. 5, no. 2, pp. 354–379, 2012.

[2] D. Iordache, J. Bioucas-Dias, and A. Plaza, "Sparse unmixing of hyperspectral data," *IEEE Trans. Geosci. Remote Sens.*, vol. 49, no. 6, pp. 2014–2039, 2011.

[3] D. Iordache, J. Bioucas-Dias, and A. Plaza, "Collaborative sparse regression for hyperspectral unmixing," *IEEE Trans. Geosci. Remote Sens.*, vol. 52, no. 1, pp. 341–354, 2014.

[4] Q. Qu, N. Nasrabadi, and T. Tran, "Abundance estimation for bilinear mixture models via joint sparse and low-rank representation," *IEEE Trans. Geosci. Remote Sens.*, vol. 52, no. 7, pp. 4404–4423, 2014.

[5] P. Giampouras, K. Themelis, A. Rontogiannis, and K. Koutroumbas, "Simultaneously sparse and low-rank abundance matrix estimation for hyperspectral image unmixing," *IEEE Trans. Geosci. Remote Sens.*, vol. 54, no. 8, pp. 4775–4789, 2016.

[6] J. Huang, T.-Z. Huang, L.-J. Deng, and X.-L. Zhao, "Joint-sparse-blocks and low-rank representation for hyperspectral unmixing," *IEEE Trans. Geosci. Remote Sens.*, vol. 57, no. 4, pp. 2419–2438, 2019.

[7] S. Gu, L. Zhang, W. Zuo, and X. Feng, "Weighted nuclear norm minimization with application to image denoising," in *Proc. IEEE Conf. Comput. Vis. Pattern Recog.*, 2014, pp. 2862–2869.

[8] D. Iordache, J. Bioucas-Dias, and A. Plaza, "Total variation spatial regularization for sparse hyperspectral unmixing," *IEEE Trans. Geosci. Remote Sens.*, vol. 50, no. 11, pp. 4484–4502, 2012.